Limnol. Oceanogr., 44(6), 1999, 1400–1414

Circulation and larval distribution in internal tidal bore warm fronts

Jesús Pineda
Biology Department, MS-34, Woods Hole Oceanographic Institution, Woods Hole, Massachusetts 02543

Abstract

Internal tidal bore warm fronts were observed during the summer of 1996 off the coast of Southern California. Warm bore fronts had concentrating currents resulting from high-frequency internal motions and from a larger two-way flow; the two-way flow featured surface currents onshore and bottom currents offshore. A sharp thermocline depression and high-frequency, large-amplitude internal motions followed the leading edge of the bore, with downwelling currents on the trailing side of the crest of the nonlinear internal waves and upwelling currents in front of the crest. Warm bores propagated onshore with a propagation speed, c, that ranged from 10.6 to 19.6 cm s^{-1}, while time-averaged frontal currents, $\bar{u}$, varied from 11.2 to 17.6 cm s^{-1} in the shallowest bin. In one out of three cases $\bar{u} > c$, which implied that there were faster currents than the rate of advance of the front and which implied that the origin of surface frontal material is behind the front, not in front of it. Three invertebrate larval taxa were found at all sites across fronts, but only two intertidal barnacles, *Pollicipes polymerus* and *Chthamalus* spp., were concentrated at the front's surface, while the subtidal bryozoan *Membranipora* spp. was not. Frontal *Pollicipes* were more concentrated than were *Chthamalus.* The frontal downwelling currents observed suggested that concentrated larvae would have to swim upward in order to maintain depth. *Pollicipes* were abundant on the offshore warm side of the fronts but were absent or rare on the onshore colder side, suggesting that the origin of frontal *Pollicipes* was behind the front, although an alternative cannot be ruled out conclusively. *Chthamalus* were more abundant at depth than at the surface at all sites except at the front, where this pattern was reversed. The origin of frontal *Chthamalus* is uncertain. *Membranipora* were more abundant on the onshore colder side of the fronts, and abundances were usually higher at depth than at surface. Lack of accumulation in this species may be due to its limited swimming capability.

Benthic communities are often composed of open populations in which recruitment is effectively uncoupled from local fecundity (e.g., Eckman 1996; Stoner et al. 1996). Because larvae of shallow-water invertebrates are generally small and cannot swim long distances, they depend on external transport mechanisms to reach adult habitats (Thorson 1950). To the extent that larval settlement and recruitment depend on external transport, these physical processes must be critically important to population dynamics. The phenomenology associated with larval transport involves larval behavior and physical transport mechanisms. Specific larval behaviors are required to exploit specific transporting or concentrating mechanisms (e.g., Scheltema 1986; Rothlisberg et al. 1995). Physical transport for nearshore species is complicated because it involves characterizing the mechanism of transport as well as its temporal and spatial variability, including the secondary flows responsible for the accumulation of larvae, responses to large-scale disturbances, and the alongshore variability.

Several studies have proposed that internal motions can transport larvae onshore, but the mechanism is ambiguous (Le Fèvre and Bourget 1992). The internal motions and the circulation have not been directly measured (Pineda 1994; Lamb 1997), and larval distributions have not been well resolved. Linear waves are unlikely to transport material, because the rate of advance of the wave, c, is much larger than the current speed generated by the waves, u. Thus, water containing the organisms of interest would be left behind by the passing wave. In addition, larval accumulation in surface features does not imply transport. As shown in models of linear internal waves, for example, cells in surface waters do not propagate with the waves. Although bands of cells are formed by internal waves and bands propagate as if the cells are advected by the waves, this illusion is caused by the constant formation of new cell bands as the model waves advance (Franks 1997). For the most part, previous descriptions of transport by surface slicks over linear internal waves have been implicitly reinterpreted to represent transport caused by nonlinear internal waves (e.g., Shanks, 1995*a,b*, and pers. comm.). This change is significant, because nonlinear waves are capable of some advection.

Shanks (1983, 1986) and Kingsford and Choat (1986) proposed that crab, barnacle, and fish larvae could be transported shoreward within slicks in convergent currents behind crests of internal waves. It was hypothesized that as internal waves move onshore, convergent currents would move too, thereby concentrating and transporting neustonic larvae onshore. Shanks (1995*b*) explained the observation that only some internal waves transport larvae (Shanks 1983), based on the equation $u \geq c$, in cases where transport occurred, but $u < c$ in situations in which transport did not occur. Lamb (1997) created a model that considers transport by nonlinear internal waves. The model predicts that these waves can transport surface plankton, particularly in the case where transport by the internal wave is ‘‘aided’’ by wind

---

Acknowledgments

D. Field helped us sample four events in challenging circumstances. K. Helfrich, K. Lamb, E. Parnell, A. Valle-Levinson, R. Geyer, R. Harbison, D. Medeiros-Bergen, J. Leichter, A. Hobday, A. Shanks, and two anonymous reviewers helped sample one event, discussed issues, commented on an earlier manuscript, and suggested the quantitative evaluation of the origin of frontal larvae. The U.S. National Science Foundation funded this project, and the Scripps Institution of Oceanography provided logistical support. This is WHOI contribution 9701.

drift or plankton swimming in the direction of propagation of the wave (*see* also Shanks 1995*b*). The model considers a system that is 300 m deep, which is deeper than most observational studies of transport by internal waves. Lamb (1997) shows that transport would be reduced in waters that are shallower than 300 m.

Internal tidal bores are another mechanism involving internal motions (Cairns 1967; Winant 1974; Holloway 1987; Helfrich 1992; Pineda 1995; Leichter et al. 1996). Bores and gravity currents ''both mark the leading edge of a continued process of mass transfer; this is not a typical feature of the behaviour of waves, the main effect of which is a transfer of energy'' (Simpson 1997, p. 95). In gravity currents and in some internal bores, $u > c$, which implies that water behind the head of a bore moves faster than does the bore itself (e.g., Winant and Bratkovich 1977; Simpson and Britter 1979). An intuitive understanding of $u > c$ in gravity currents can be obtained by considering that when the head of a gravity current penetrates ambient water of different density, head water is lost because of mixing with ambient water; since the lost mass can only be replaced by water behind the head, $u > c$. Internal tidal bores in Southern California occur in groups of two to nine events in spring and summer, when the water column is well stratified. These groups of events are more probable 7–12 and 19–24 d after the new moon, although the first event in a series is unpredictable in the short term (Pineda 1995). Internal tidal bores have superimposed high-frequency internal motions (Cairns 1967; Winant 1974).

Just as internal waves and tides have crests and troughs, nearshore internal tidal bores occur in two phases. In the first phase, a cold-water bore is advected shoreward, displacing warm water offshore and creating an imbalance in hydrostatic pressure between heavier inshore water and lighter offshore water. A front forms between the inshore cold water and the displaced offshore warm water. In the second phase, cold water recedes offshore because of its density, currents reverse, and a ''warm'' internal bore returns, pushing the front all the way to the shore (Pineda 1994). Some events feature a single semidiscrete temperature front, whereas others feature more. There is another compatible and complementary way to understand these phenomena. In this view, internal tides have propagating crests and troughs, and while the colder water at the nearshore represents the crest, the warm water would follow, representing the trough (e.g., Arthur 1954; Holloway 1987). This view does not invoke explicitly cross-shore pressure gradients. In the nearshore, however, a pressure gradient must exist when the crest of the internal tide is inshore and the trough offshore. In both views, diurnal and semidiurnal temperature variability in the nearshore would represent the flux and reflux of the internal tide. It has been proposed that the cold phase of internal tidal bores transports water-column taxa onshore (Pineda 1991; Leichter et al. 1998), whereas the warm phase transports neustonic larvae (Pineda 1994).

This contribution focuses on the warm bore fronts. While Pineda (1994) broadly described internal bore warm fronts and presented evidence supporting the hypothesis that these fronts transport fish and crab neustonic larvae onshore, several puzzling observations remained unanswered. One issue is that while it was proposed that these fronts would transport neustonic larvae, qualitative plankton observations showed that these fronts also contained high concentrations of nonneustonic barnacle cyprids. Another intriguing observation was that the initial rise in surface-water temperature observed with the front was followed by a drop, which suggested that strong upwelling occurred shortly after the front. Other important unanswered questions required elucidation of the mechanism of frontal larvae concentration and of the overall circulation patterns in the fronts. In this contribution, the following questions are addressed. What are the patterns of circulation in internal bore fronts? Do different taxa accumulate differently in the fronts? Do these larval taxa have similar horizontal and vertical surface distributions across the fronts? Do patterns of circulation support any given hypothesis of larval accumulation? And finally, can circulation patterns explain accumulation of water column and neustonic taxa?

Methods

Several fronts were sampled in the summer of 1996 off La Jolla, Southern California, ~1–1.5 km southwest of the Scripps Institution of Oceanography pier. Some fronts were sampled for plankton, temperature, and currents, whereas others were only sampled for plankton or for temperature and currents. All events revealed diurnal/semidiurnal temperature periodicity similar to that associated with other internal tidal bore events in this region.

Large internal bores are unpredictable in the short term, and successful larval sampling of these events requires a sampling scheme that reacts to the events (Pineda 1994). Adaptive sampling of temperature, currents, and larvae started when a large cold bore was detected at the nearshore with quasi–real-time temperature sensors. Cold water anticipated a front, which followed a few hours later. In anticipation to the fronts, temperature loggers and a current meter were deployed, and plankton sampling was initiated.

Temperature and current measurements—Temperature and currents were measured with moored instruments in ~10–14 m of water in various short-term deployments. A cross-shaped array of six temperature moorings (M1–M4 and MA and MC) had adjacent moorings separated by 30 m; the array had axes parallel and perpendicular to isobath contours, which in this area run in a north–south direction (Fig. 1). A submarine canyon offshore of the moorings is found at approximately >35–45 m in depth. Temperature moorings were set tight by increasing subsurface float buoyancy in order to diminish bending by currents. A current-meter mooring was set up generally midway between M2 and M3 or close to M2. Not all moorings recorded observations in all events, and almost all observations described here were obtained with the M2 mooring, with other mooring observations used only to obtain the direction of propagation and the phase speed (*see below*). Analysis of other temperature observations that are irrelevant to this study will be presented elsewhere. The M2 mooring was in ~11 m of water and had Onset Stowaway temperature loggers at 1, 3, 5, 7, and 9 m above the bottom (mab) and one floating log-

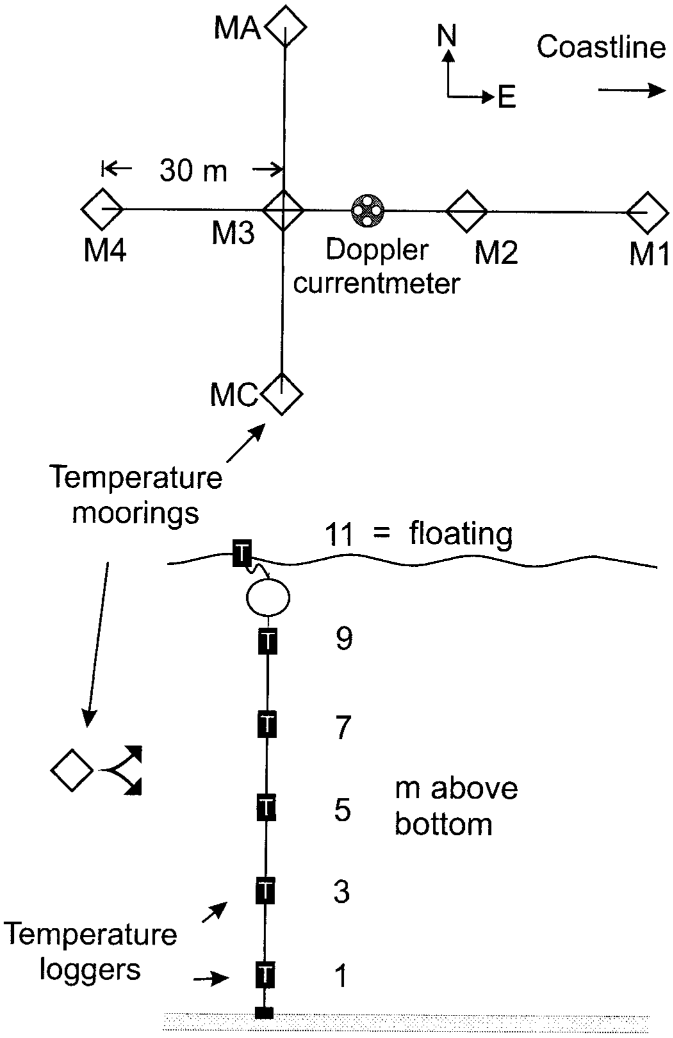

Fig. 1. Schematic representation of the experimental array.

ger as well (~11 mab). Temperature loggers recorded temperature at 5-s intervals in one event and at 8-s intervals in the rest of the events. The 1,200-kHz RDI Workhorse Doppler current meter measured currents at 10-s intervals, with bin sizes of 0.50, 0.60, or 0.65 m in different events. Bins closest to the surface were discarded because they were contaminated with surface phenomena, with depth of the top bin determined by environmental conditions. All temperature data were low pass filtered with a five-point (25-s) or six-point (48-s) running mean filter, whereas the currents were filtered with a five-point (50-s) filter.

In one event, temperature and depth profiles were obtained across a front with a conductivity, temperature, and depth profiler (CTD); profiles were obtained within ~1 h. The conductivity sensor did not operate properly, and no conductivity profiles were obtained.

Bore front phase speed and direction of propagation—Bore front phase speed (e.g., the speed at which bore fronts propagate) and the direction of propagation were calculated using temperature–time series in three moorings on 29 June and on 2, 3, and 13 July 1996. This analysis assumes that the bore front was linear, that the direction of propagation was perpendicular to the crest of the bore front, and that the speed of the bore front was constant within the three moorings (e.g., Ufford 1947; Lee 1961). Small spacing within moorings helped justify these assumptions. The direction of propagation, θ, relative to the MC–M2 line was calculated as follows:

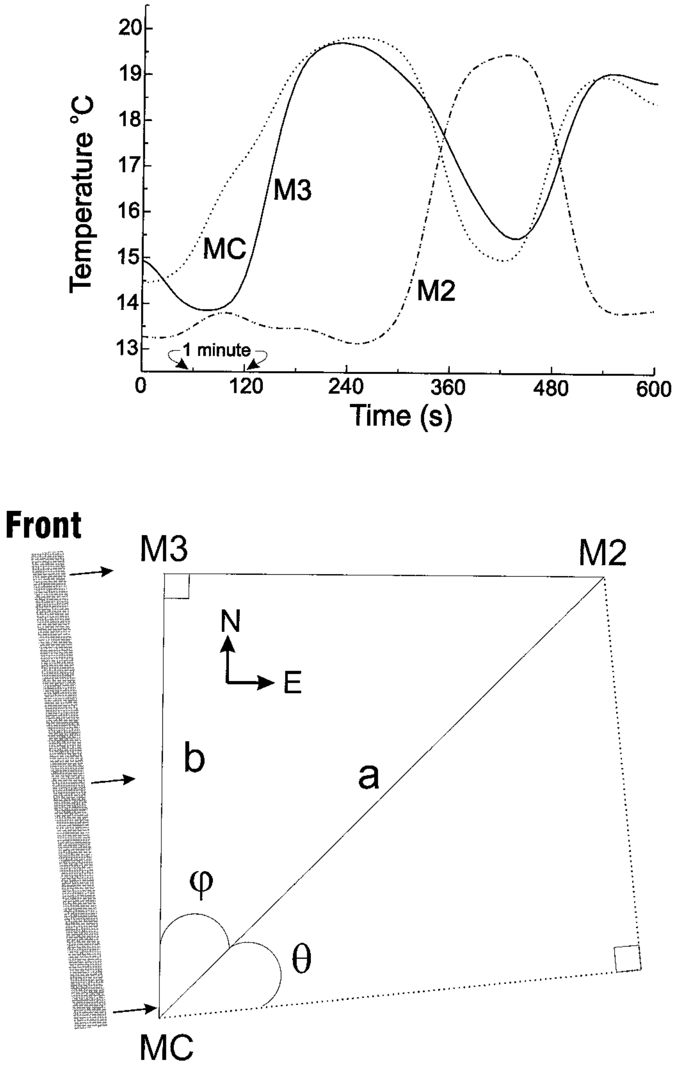

Fig. 2. Temperature plots in single 5- or 7-mab temperature loggers at MC, M3, and M2 and example of array used for calculating propagation speed and direction of propagation. The gray bar is a schematic representation of a front approaching the array.

$$\theta = \tan^{-1}\left(\frac{\dfrac{aT_{M3-MC}}{bT_{MC-M2}} - \cos\varphi}{\sin\varphi}\right) \tag{1}$$

where a is the distance between MC and M2 and b is the distance between MC and M3 and where T_{Mx-My} constructions indicate time lags between temperature traces in moorings M_x and M_y, obtained from cross-correlation (Fig. 2, top panel). For example, on the July 3 front, $b \approx 3{,}000$ cm; a

$\approx$ 4,243 cm; $T_{M3-MC} = 16$ s; $T_{MC-M2} = 168$ s; and $\varphi = 45°$ (Fig. 2). This yields $\theta \approx -39°$ relative to MC−M2, or $\theta' = 6°$ relative to the east–west axis. Propagation speed is calculated as

$$c = \frac{a \cos \theta}{T_{MC-M2}} \tag{2}$$

yielding $c = 19.6$ cm s^{-1}.

Current rotation in the direction of front propagation—The Doppler current meter outputs vertical, east and north currents. In order to obtain the horizontal component in the direction of front propagation, east–north currents were "rotated" according to propagation direction θ', as determined above. A second criterion for rotating the currents was derived to compare it with θ'. This criterion was based on the finding that in this region, the spring and summer water column is two layered, and internal motions behave according to internal mode 1—currents in the bottom and surface layers move in opposite directions (Winant and Olson 1976; Winant and Bratkovich 1981). This finding was taken as an assumption for this analysis. A second assumption was that in the events, the dominant forcing was due to the internal bore, whereas other forcings, such as wind or the surface tide, were negligible. Assuming these two premises, a profile of horizontal currents from the bottom to the sea surface would show opposite currents in the bottom and upper layers: large variability of the horizontal currents in the vertical. This two-way pattern will be more obvious when currents are rotated in the direction of propagation of the events, compared with currents rotated with an arbitrary angle. Currents rotated in the direction of propagation should then exhibit maximum variability or maximum standard deviation with depth (*see below*).

In each one of the four events, approximately a 30-min time series of frontal horizontal currents was rotated every 1° from −90° to 90°, relative to the east (−90° is south; 90° is north). The time-averaged current, $\bar{u}_i$, for each depth bin i was then obtained for each rotation. For $i = 1, 2, \ldots b$, where b is number of bins measured (13–17; also b = shallowest bin),

$$\bar{u}_i = \frac{\sum_{t=0}^{n} u_t}{n} \tag{3}$$

The time at which the front starts is $t = 0$, and n is number of observations corresponding to about 30 min of currents. For currents measured at 10-s intervals, this corresponds to 180 observations. For each 1° rotation, the vertically averaged currents, $\bar{u}_z$, and the standard deviation s_z of the vertically averaged currents were then obtained:

$$\bar{u}_z = \frac{\sum_{i=1}^{b} \bar{u}_i}{b} \tag{4}$$

$$s_z = \sqrt{\frac{\sum_{i=1}^{b} \bar{u}_i - \bar{u}_z}{b - 1}} \tag{5}$$

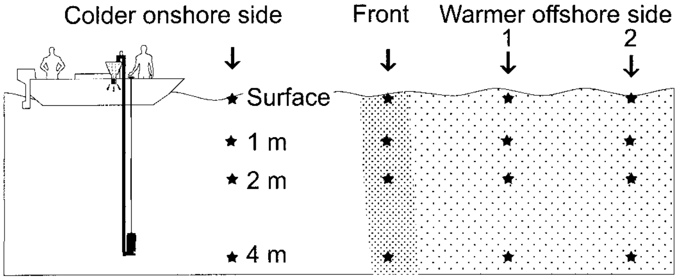

Fig. 3. Schematic representation of larval sampling.

$R_{\mathrm{smax,}}$ the rotation corresponding to maximum s_z, should give the direction of front propagation.

Larval measurements—Plankton were pumped at four sites and at four depths across the fronts using an Ebara semivortex AC pump on five separate dates: 1, 3, 5, 7, and 19 July 1996. There were two sites on the offshore warm side of the fronts ("offshore" 1 and 2), one site at the front, and one site on the onshore colder side (Fig. 3). Fronts were identified by an accumulation of surface material and horizontal changes in temperature that were >0.5°C over a few meters. Offshore 1 sites were at 200–500 m from the front, and offshore 2 sites were >900 m from the front. The onshore sites were at ~100–500 m from the fronts. Bottom depth and sampling position varied with the fronts, but colder samples were always onshore and, therefore, in shallower water than were the other samples. Sampling depths were surface (0–0.4 m) and 1, 2, and 4 m below the surface. One cubic meter was pumped in about 3.9 min, with each site taking less than 20 min. The onshore site was always sampled first and the offshore 2 site last. Sampling drifted with the frontal feature and with the flow. Some samples on the onshore sites were obtained at fixed locations in order to avoid approaching shallow water (<6 m).

Plankton was filtered using a 106-μm net and was then analyzed with a microscope, and barnacle *Chthamalus* spp. and *Pollicipes polymerus* cyprids and bryozoans, *Membranipora* spp. cyphonautes, were counted. *Chthamalus* cyprids were not identified to species, but *Chthamalus fissus* is by far the most abundant barnacle in Southern California, with *Chthamalus dalli* and an unnamed southern *Chthamalus* being rare (W. Newman pers. comm.; Ricketts and Calvin 1968). For the cyphonautes, Yoshioka (1982) found that most larvae in La Jolla, California, were *Membranipora membranacea.* For each taxon, number of larvae sampled on each date was converted to percentages by dividing the number of larvae in each depth and site by the total number of larvae. Percentages in each depth and site were then averaged for the five dates. This procedure yields percentage data that are independent from overall abundance, which varied greatly among dates (*see below*). The larval data were analyzed with a nonparametric analogue of two-way analysis of variance, the Scheirer–Ray–Hare test (Sokal and Rohlf 1995).

Results

During nonbore conditions, the water column showed strong two-layer thermal stratification, a structure typical of

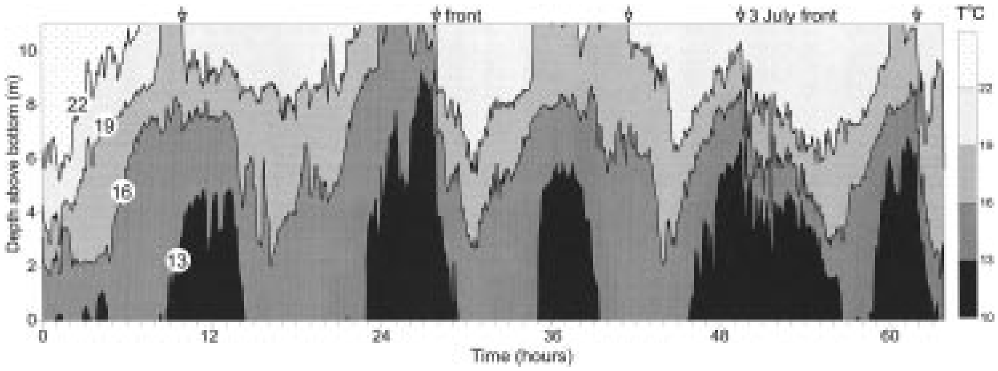

Fig. 4. Interpolated temperature observations in M2 mooring. Temperature loggers at 1, 3, 5, 7, 9, and ~11 (surface) m above bottom.

Southern California waters during the summer (Winant and Bratkovich 1981). Several internal tidal bore events were detected in late June and early July 1996 (Fig. 4). Cold and warm water alternate in about a 12-h period throughout the entire water column. Cooling of the water column is interpreted as advection of thermocline water by large internal tidal bores, whereas warming results as cold water recedes offshore and as warmer water returns. Arrows point to the internal bore warm fronts discussed in this paper, and the front at about 50 h is the July 3 front described below. Interpolated temperature across an internal bore warm front from four temperature profiles on the July 3 event demonstrates a surface-temperature gradient of greater than 3°C, with colder water inshore and the 20, 19, 18, and 17°C isotherms intersecting the sea surface (Fig. 5). Cast No. 2 was at the front, and casts 1 and 4 were separated by ~650 m in the cross-shore x-axis, measured with a differential global-positioning system. Cast number rather than distance was plotted in the x-axis, because the front was moving shoreward and the casts were far from synoptic. Assuming a constant salinity of 34 parts per thousand, the cross-shore gradient in the density of the top 7 m, the depth of the inshore station, was 0.00135 kg m^{-4}.

Current rotation in the direction of front propagation—The time-averaged currents (~30 min) rotated according to θ' showed strong vertical shear for the June 29 and July 3 and 13 events, with offshore currents in the bottom layer and onshore currents in the top (Fig. 6). A different pattern was obtained on 2 July 1996, with slower onshore and offshore currents, and two current reversals with depth. For 29 June and 3 and 13 July 1996, onshore upper-layer currents increased monotonically with distance from the bottom, with the top bin currents, $\overline{u}_b$, having the highest onshore values. Lower layer currents increased with depth, but mean currents at the deepest bin were not the fastest offshore currents. Fastest offshore currents occurred at a distance from the bottom, which is consistent with the fact that bottom friction slows the currents in the bottom layer.

The s_z curves were similar for 3 and 13 July and 29 June 1996, and they contrast sharply with that of 2 July 1996, which featured the smallest s_z and s_z-range of all events (Fig. 7). On 3 and 13 July and on 29 June 1996, θ' and R_{smax} agreed well, while on 2 July 1996, there was a large discrepancy (Table 1). On 2 July 1996, strong alongshore north currents, which were presumably unrelated to the bore, dominated the flow, and vertical currents differed from two-layer mode-1 variability (e.g., currents were not two-way). $\overline{u}_b$ is not presented for this date because it violated the assumptions of the analysis; it was larger than c on 29 June 1996 and smaller in the two other events. $\overline{u}_b$ depth was ~9.5 mab on 29 June, ~9 on 3 July, and ~8.4 on 13 July 1996. $\overline{u}$ at the sea surface may had been higher than $\overline{u}_b$, since the layered structure gives uniform velocity with height in each

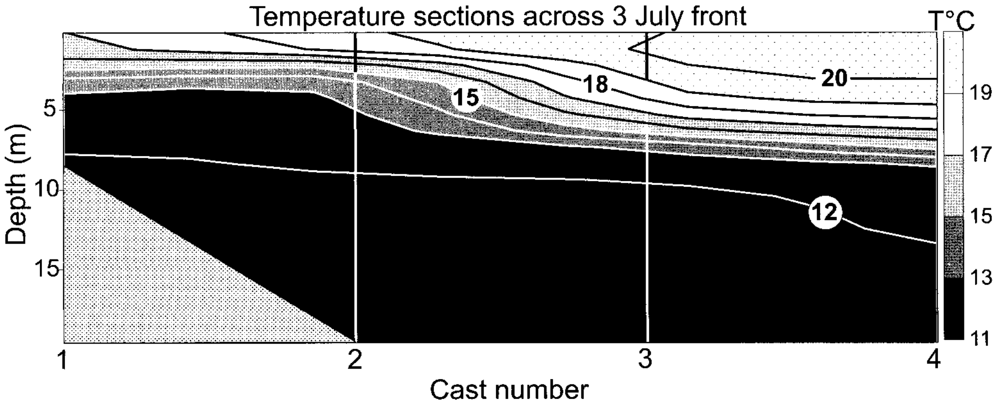

Fig. 5. Interpolated temperature from four CTD profiles on 3 July 1996.

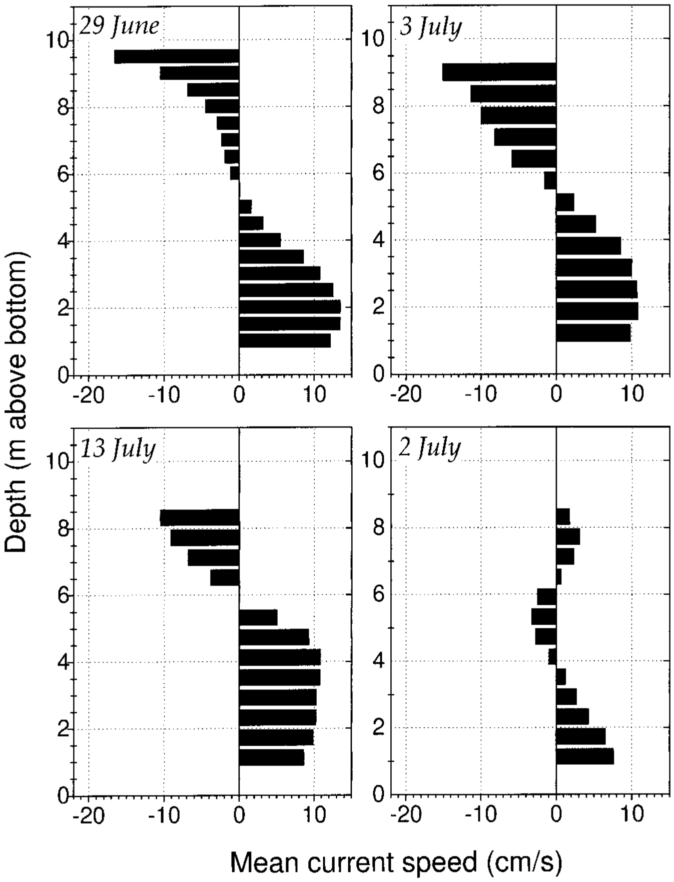

Fig. 6. Time-averaged horizontal currents rotated according to θ' (*see Table 1*). Negative currents are onshore, and positive currents are offshore. Currents closest to the surface are $\bar{u}_b$.

layer. The June 29 event featured increased shear toward the surface (Fig. 6), and it may be considered that this was caused by onshore winds. However, winds measured at the Scripps Institution of Oceanography pier during this event were very weak and were blowing contrary to the direction of the surface currents.

Temperature and rotated currents—Rotated currents and M2-interpolated temperature were plotted for the July 3 and 13 warm bore events (Figs. 8, 9). Currents were advanced 100 s on 3 July 1996 because the current meter was moored ~15–20 m seaward of M2. (The July 3 event was also plotted on other scales in Figs. 4 and 5.) The July 3 event reveals cooling of the water column (about 11 m; Fig. 8, upper left) and, at about 86 min, a sudden 1°C rise in surface temperature manifested as a shoreward moving surface front. Cooling before the front was typical in all events. Circulation patterns show weak horizontal and vertical currents in front of the front and stronger vertical and horizontal currents behind the front. Behind the front, bottom and surface currents were generally opposite, with the surface-water layer migrating shoreward and the deeper water receding offshore. With stronger onshore currents close to the surface on the offshore warm side of the front and weaker on the onshore cold side, surface material, which consists of kelp, grass, and other floating material, accumulated at the front. The front featured a sharp 3-min thermocline depression with loop current patterns, down on the onshore cold side of the front and up on the offshore warm side. Some surface material must sink with the downwelling surface currents, whereas upwelling currents explain cooling behind the front on the offshore warm side, a feature often observed in these events. The floating temperature instrument also detected two other drops of about 0.5°C, corresponding to peaks of ~5-min period internal motions following the fronts (Fig. 8, ~104 and 111 min). The wave height of these motions was > three-quarters of the water column height, which demonstrates strong nonlinearity. There were weak current relaxations or reversals, corresponding to peaks of internal motions (Fig. 8, ~90 and 105 min). The water column was strongly sheared at the troughs of the higher frequency internal mo-

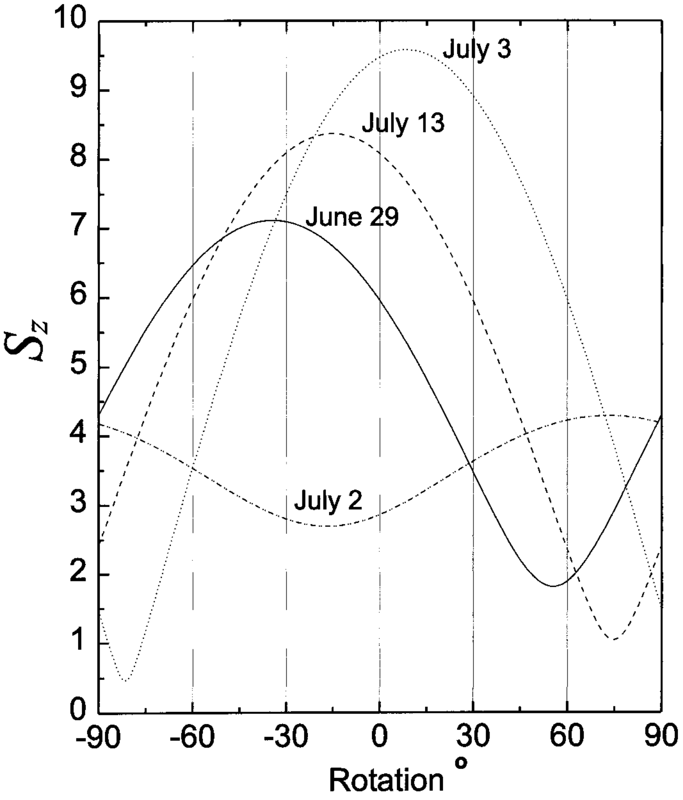

Fig. 7. Standard deviation s_z of currents rotated from −90° to 90°.

Table 1. Phase speed c, mean onshore rotated current speed in upper bin $\bar{u}_b$, direction of propagation θ', and rotation at maximum standard deviation R_{smax}. c and θ' were derived from temperature, whereas $\bar{u}_b$ and R_{smax} were derived from currents.

Date	c (cm/s)	$\bar{u}_b$ (cm/s)	θ' (degrees)	R_{smax} (degrees)
June 29	14.1 cm/s	17.6 cm/s	−31°	−35°
July 3	19.6 cm/s	16.0 cm/s	6°	8°
July 13	14.8 cm/s	11.2 cm/s	−20°	−15°
July 2	10.6 cm/s	—	22°	73°

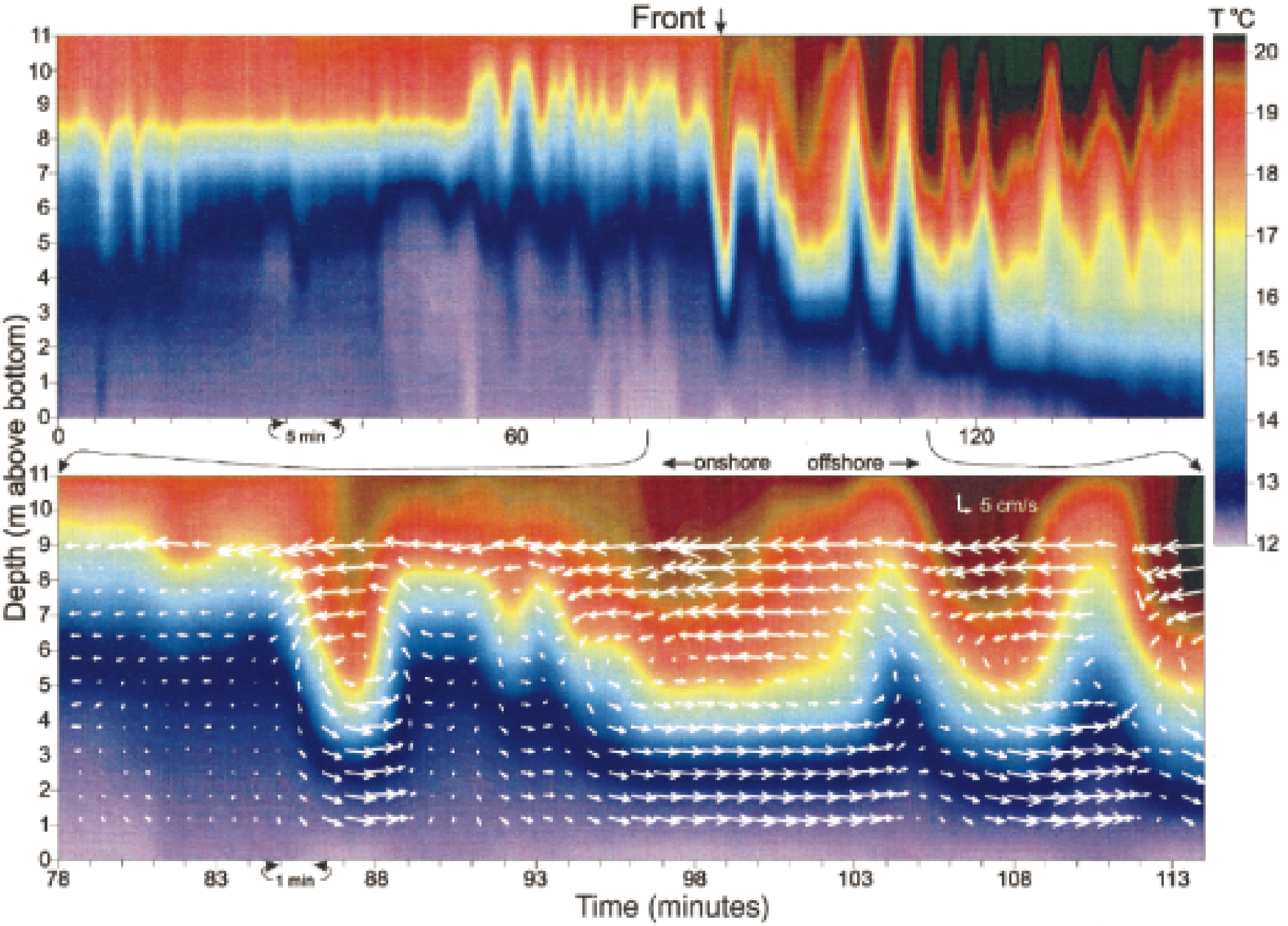

Fig. 8. Interpolated temperature and vertical/onshore–offshore current vectors on 3 July 1996. Positive is offshore. Horizontal currents were rotated $\theta' = 6°$ with respect to the east–west axis. The lower panel is an amplification of the upper panel. Temperature loggers were at 1, 3, 5, 7, 9, and ~11 (floating) m above the bottom, whereas the Doppler current meter was at the bottom, about 15 m offshore from the temperature mooring. Currents were advanced 100 s to match temperature. Temperature and currents were sampled at 8-s and 10-s rates, respectively. Current vectors are shown every 40 s, and the top bins were removed as they were contaminated by surface phenomena. Missing current vectors around 111 min did not pass several acoustic data quality criteria or were removed from raw data when vertical currents were $> |35|$ cm s^{-1}.

tions. The peaks of the high-frequency motions delineate circulation cells along the troughs, with downward currents at the back side of the onshore peaks and upward currents at the front side of the offshore peaks (Fig. 8; downward at ~94, upward at ~103 min). Surface slicks following the fronts were often observed, and concentrations of surface material were occasionally observed there. Slicks most likely coincided with the downwelling currents on the trailing side of the crest of the high-frequency motions. Small high-frequency features were also observed before the front.

The warm bore event on 13 July 1996 did not feature a surface-temperature increase (Fig. 9). Vertical circulation patterns were generally similar to those of the July 3 event. There was an offshore flow in the upper layer in front of the bore, which changed to onshore with the bore. The surface offshore flow in front of the bore did sink just before 10 min and continued offshore in the bottom layer. After 10 min, the surface layer moved onshore and the bottom layer offshore. The water column was strongly sheared, with a zone of weak currents corresponding to the ~16–17°C contours and strong opposite currents above and below. As the isotherms moved up and down with the high-frequency internal waves, the zone of minimal currents generally did follow up. Unexplained fast currents, maybe an overturning event, occurred at ~30 min.

Larval measurements—Pollicipes cyprids were concentrated in the front, with highest percentages overall at the surface and at 1 m; few or no larvae were found on the onshore colder sides of the fronts, whereas percentages on the offshore warmer sides were higher at surface than at depth (Fig. 10). *Chthamalus* cyprids concentrated at the fronts' surfaces, although less than were the *Pollicipes;* the vertical distribution at the front contrasts with the onshore

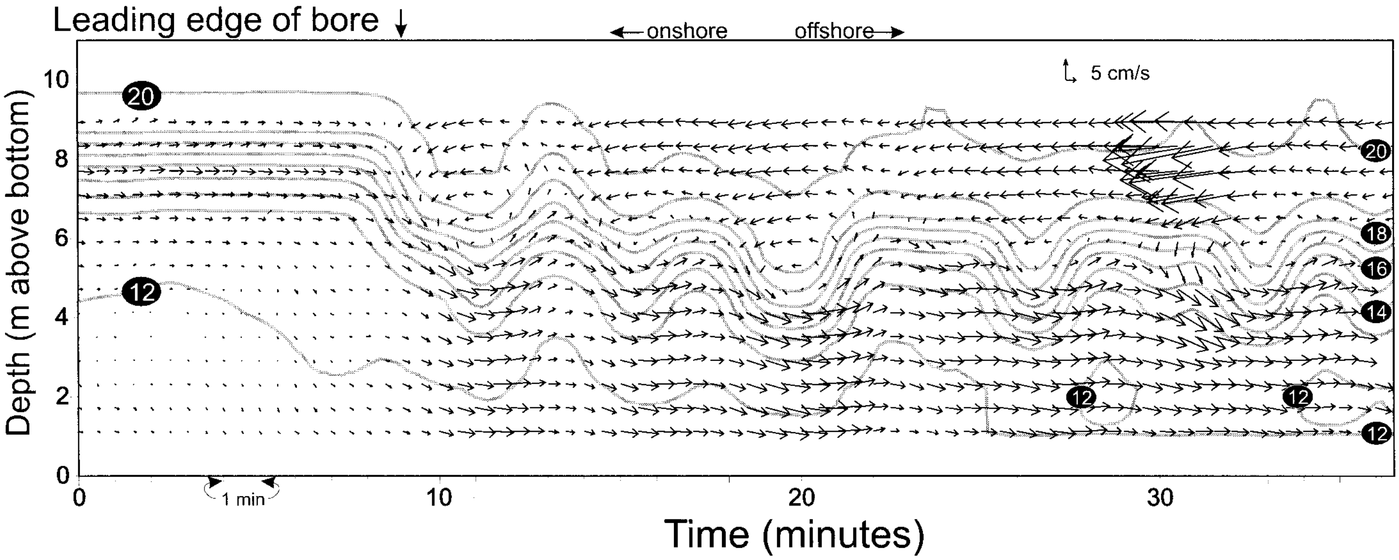

Fig. 9. Interpolated temperature contours and vertical/onshore–offshore current vectors on 13 July 1996. Positive is offshore. Horizontal currents were rotated $\theta' = -15°$ with respect to the east–west axis. Doppler current meter was at about the same location as the temperature mooring. See Fig. 8 legend for other details.

colder and offshore warmer sides, where percentages were higher at 4 m than at the surface (Fig. 11). *Membranipora* cyphonautes did not concentrate at the fronts; percentages were generally higher on the onshore colder side of the front and at 4 m, with the exception of a high value at the surface in the offshore 2 side (Fig. 12). Vertical distributions for the three taxa on the offshore warm side of the fronts were more variable than they were at the fronts, with some unexplained reversals to the general patterns in Figs. 10–12 at given dates. Overall, *Membranipora* were more abundant than were *Pollicipes,* and *Pollicipes* were more abundant than *Chthamalus,* with $\bar{x} = 24.3$, 11.5, and 3.4 larvae m^{-3}. *Pollicipes* abundance onshore of the front was zero on 5, 7, and 19 July 1996 (Fig. 13). *Membranipora* abundance peaked at most sites on 5 July 1996, a trend not observed in the barnacles. On 7 and 19 July 1996, *Membranipora* showed moderate to low abundances at all sites, whereas the frontal abundances of the two barnacle taxa peaked. There were very few larvae overall on 3 July 1996. The nonparametric test showed that there was evidence supporting the idea that ranks were nonrandomly distributed by depth for *Chthamalus* and *Membranipora,* whereas *Pollicipes* ranks were nonrandomly distributed by site (Table 2).

Discussion

Internal tidal bore warm fronts—The internal bore fronts discussed here are similar to events previously described by Arthur (1954), Winant and Olson (1976), and Pineda (1994). In contrast to present observations, Winant and Olson (1976) measured highest current velocities in the middle of the water column, thus supporting the idea of a three-layer model. The evidence suggests that the events discussed here are associated with the flux and reflux of the internal tide. Masses of heavier and lighter water alternating at a periodicity of ~12 h imply that the nearshore waters are replaced about every 6 h (Fig. 4). The cross-shore uplifting of the thermocline (Fig. 5) suggests the observed two-way flow (Fig. 6). The time scale of the two-way currents observed here (>30 min) and previously (several hours, Winant and Olson 1976; Pineda 1994) also indicates that these events are related to the internal tide.

Holloway (1987, 1991) depicted thermocline oscillations such as those in Fig. 4 as the internal tide and sharp thermocline features as the leading face of the internal tide, propagating as an internal bore. In particular, Holloway's (1987) fig. 2 shows a propagating sharp feature, ''an hydraulic jump (or internal bore),'' followed by a packet of large-amplitude, high-frequency internal waves. The high-frequency internal waves trailing the bore fronts (Figs. 8, 9) appear to be the same phenomena that Holloway (1991) described as being associated with the dissipation of shoreward propagating internal tides.

The July 13 event had no surface-temperature front (Fig. 9). The strong concentrating circulation in the leading edge of this event implies the presence of surface slicks and the accumulation of surface material, a phenomenon often observed in the field (Pineda pers. observ.). Without water-column observations, this advective event would visually appear (exactly) to be a train of surface slicks over internal waves, independent from the internal tidal bore. This result is a warning for observers who are attempting to identify internal wave slicks with visual observations alone, and it underscores a problem found in several previous studies of internal wave surface slicks. The identification of such phenomena must be based on water-column measurements.

The adaptive sampling protocol in Pineda (1994) and in this study is hypothesis dependent, based on the conjecture that the cold water advected by internal tidal bores anticipates the arrival of the internal bore warm fronts. Sampling larvae and high-frequency physical properties in large internal tidal bores is challenging, because these phenomena are

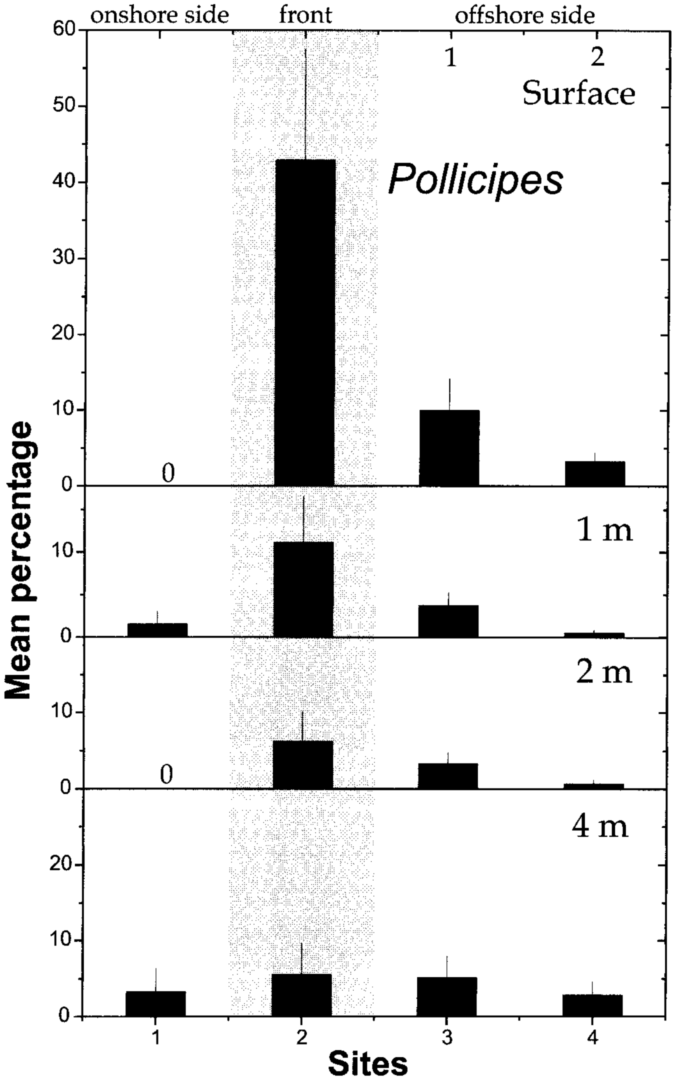

Fig. 10. Mean percentage and standard error for *Pollicipes polymerus* cyprids, sampled on 1, 3, 5, 7, and 19 July 1996.

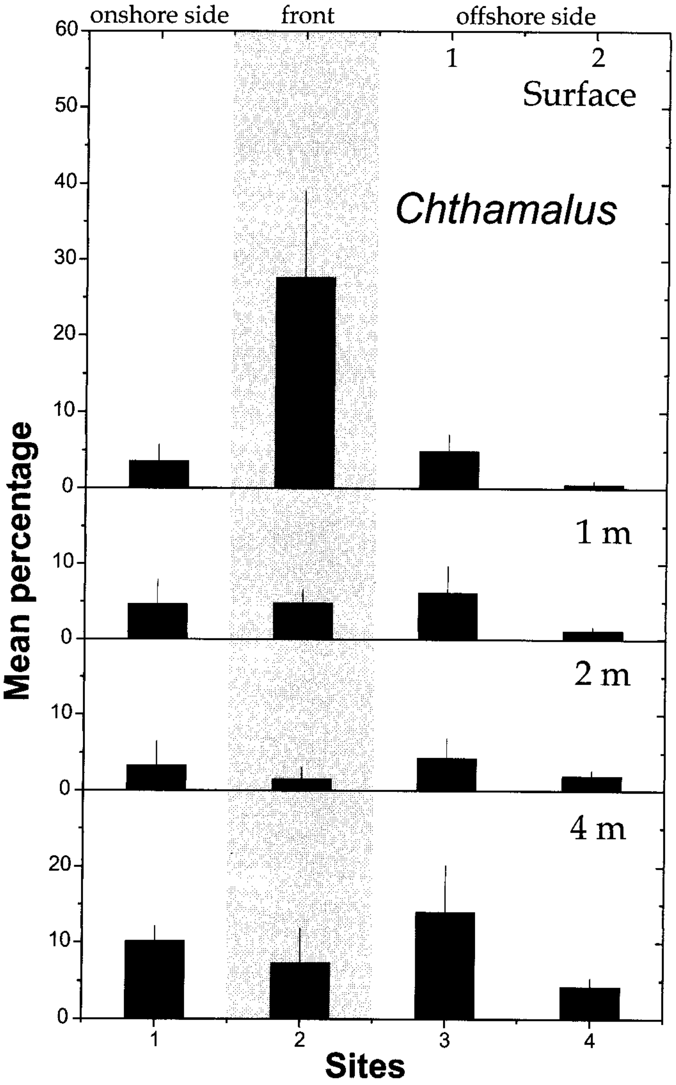

Fig. 11. Mean percentage and standard error for *Chthamalus* spp. cyprids sampled on 1, 3, 5, 7, and 19 July 1996.

events; although more probable in certain seasons and days of the lunar cycle, the first event in the series is unpredictable in the short term (Pineda 1995). For example, a systematic sampling protocol contrasting spring versus neap internal motions would probably miss the warm bores. An adaptive sampling scheme is required to obtain relevant biological observations, because samples have to be obtained from the ephemeral fronts. This scheme is also currently required to obtain high-frequency physical observations, unless moored instruments are replaced frequently or unless data are transmitted in real time. (For example, the temperature loggers with a ~32,000 data capacity would fill their memory in ≈3 d when set at an 8-s sampling interval.)

One goal of this study was to obtain field observations of larval distribution and water circulation in internal bore warm fronts; a schematic model of the circulation in these events is presented in Fig. 14. This endeavor is critical for quantitative modeling of these phenomena. To my knowledge, no other study has resolved this circulation under field conditions.

Phase–current speed relationships and transport—In the events discussed here, the new warm water detected at the surface with the floating temperature logger demonstrates mass transport. Necessarily, for the top layer, $u \geq c$. This onshore transport is dependent on depth, as onshore u decreases with depth. For the middle and bottom water column, there is little onshore transport, or transport is directed offshore. Currents at the sea surface could not be measured, and direct measurements of u at the surface are thus unavailable. The top-bin mean current $\overline{u}_b$ is the closest current to the surface that can be compared with c, and $\overline{u}_b$ was larger than c on 29 June but smaller on 3 and 13 July 1996. On the other hand, there was more shear closer to the sea surface on 29 June than on 3 and 13 July 1996 (Fig. 6). It is not known what caused these differences in $\overline{u}_b$, c, and shear; wind does not appear to be a factor, as June 29 winds were

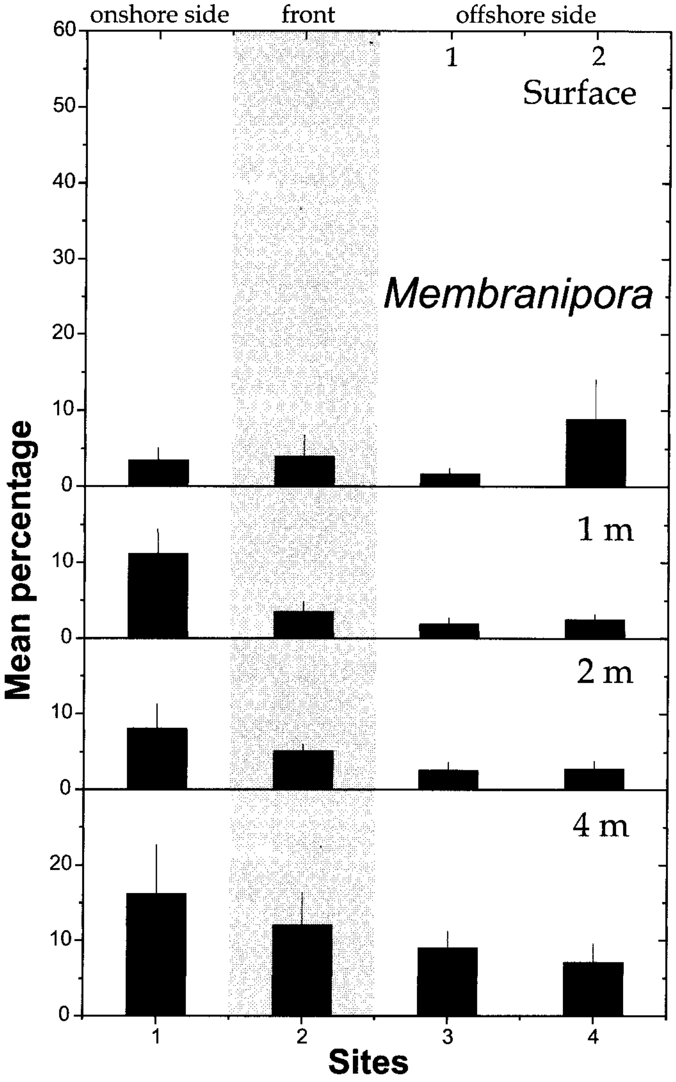

Fig. 12. Mean percentage and standard error for *Membranipora* spp. cyphonautes sampled on 1, 3, 5, 7, and 19 July 1996.

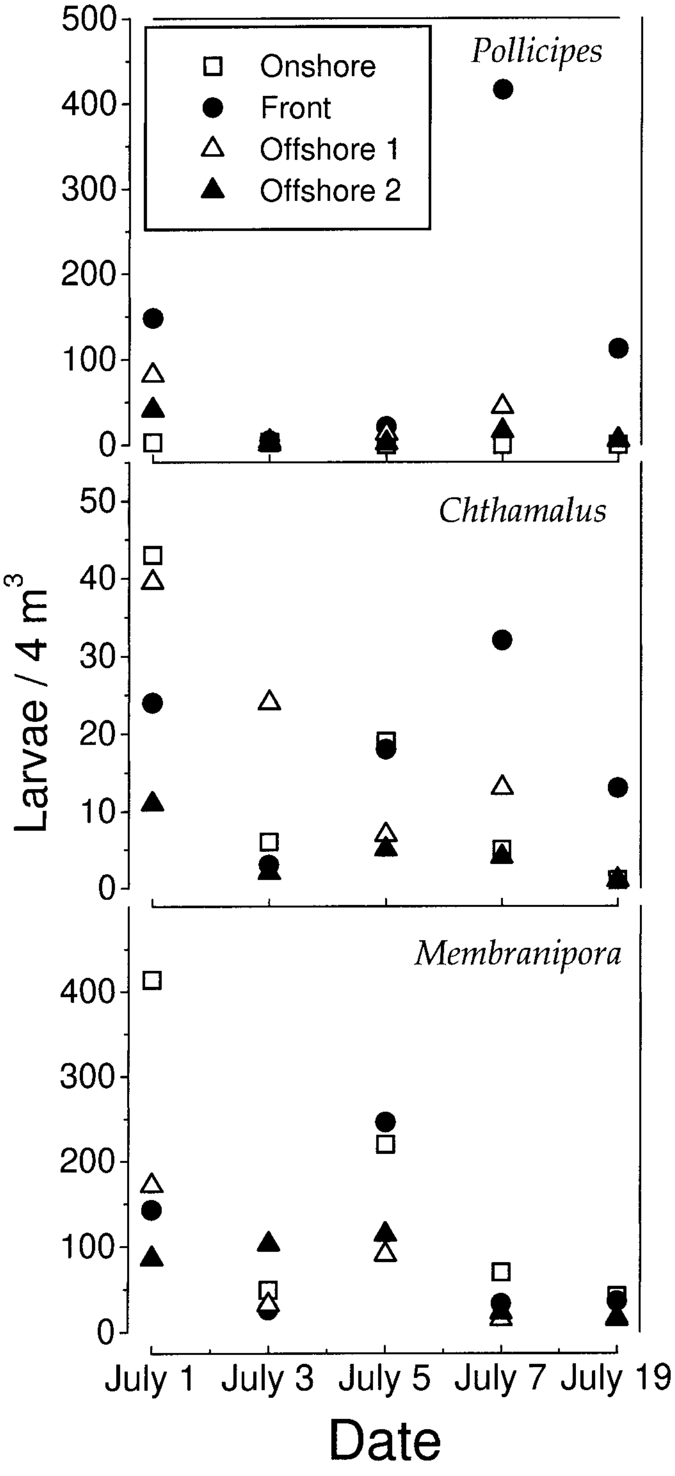

Fig. 13. Total number of larvae per 4 m^{-3} sampled per date per site. Sites include all depths.

weak and blowing contrary to the direction of the surface frontal currents. Because only three events were sampled, a statement about the frequency of events during which there is more or less shear would be premature.

The hypothesis of plankton accumulation proposed below depends on $u > c$. Several lines of evidence and arguments support $\bar{u} > c$ close to the sea surface. (1) Results show that $\bar{u}_b - c = 3.5$ cm s^{-1} on 29 June 1996. This is a conservative estimate, as there is a tendency for the currents to increase with decreasing depth, and the 3.5 cm s^{-1} value was obtained at a distance from the surface. (2) An important conjecture is that (i) if the front is associated with an increase in water temperature, and (ii) if there is no differential heating in the cross-shore axis, it then follows that (iii) there is mass transport of warm water. Assuming (iii) and (iv) (that the front is associated with the warm water), it then follows, necessarily, that somewhere $\bar{u} \geq c$. $\bar{u}$ cannot be less than c, because this would imply that the warm water would be left behind by the faster front. (3) $\bar{u} > c$ is supported by a two-dimensional model (Simpson and Britter 1979) and laboratory experiments that "appear to model closely the behavior of a gravity current of freshwater moving along the free surface above saline surroundings" (Simpson 1982; *see also* Winant and Bratkovich 1977). This model system is then analogous to the internal tidal bore warm fronts. Field ob-

Table 2. Scheirer-Ray-Hare test on larval percentages. Ns tested for $\alpha = 0.05$.

Larvae	H statistic	Significance test
Chthamalus		
Site	5.963	NS
Depth	10.532	$P < 0.05$
Site·depth	10.642	NS
Pollicipes		
Site	28.762	$P < 0.001$
Depth	4.987	NS
Site·depth	6.710	NS
Membranipora		
Site	6.866	NS
Depth	16.095	$P < 0.01$
Site·depth	10.070	NS

servations of a sea-breeze front, another type of gravity current, but one with different boundary conditions than are associated with the warm bores, also support this phenomenon (Simpson and Britter 1979).

The equation $u \geq c$ may be counterintuitive for students who are used to wave models, but this is a result that is often observed and substantiated by experiments, field observations, and theory on gravity currents. That u is faster than c implies that currents transport particles toward the front at a rate faster than the propagation speed of the front. At the front, onshore currents turn, and water flows downward. Floating particles transported from behind the front toward the front would be trapped at the downwelling site. The system is analogous to a forward-moving conveyor belt (Fig. 14).

Larval vertical and horizontal distribution—Previous work explained that water-column taxa would be transported by the colder water phase, whereas strictly neustonic taxa would be transported by the warm internal bores (Pineda 1991, 1994; Leichter et al. 1998). This study shows that water-column taxa such as *Chthamalus* cyprids and nonstrictly neustonic *Pollicipes* cyprids can both be transported by the warm bores. My results cannot differentiate the relative importance of the two phases, but a greater concentration and abundance of *Pollicipes* and higher percentages at the surface on the offshore warm side of fronts suggest that surface fronts may be more important for this species than for *Chthamalus.*

Patterns of larval abundance across the fronts and from the surface to 4 m differed among the three larval taxa, which demonstrates the importance of resolving the larval taxa to the lowest taxonomic level. While *Pollicipes* accumulated at the front, *Membranipora* did not. *Chthamalus* ranked first in three out of the five dates in the surface of the fronts, which suggests accumulation. However, the results of the statistical test for differences across sites were nonsignificant. Patterns of accumulation may be related to larval behavior, as has previously been hypothesized (e.g., Shanks 1983).

Pollicipes tended to be more abundant at the surface than at depth, and this trend was enhanced at the fronts; to my knowledge, there is no published information about *Pollicipes'* vertical distribution. *Membranipora* cyphonautes were more abundant at depth than at the surface, a result that is consistent with that of Yoshioka's (1982) study. *C. fissus* is by far the most abundant barnacle in Southern California, and the nearshore barnacle cyprid larvae center of abundance in a Southern California location was at depth (Barnett and Jahn 1987). *Chthamalus* cyprid abundances on the offshore warm side of the fronts were higher at 4 m than at the surface but were reversed at the fronts. This implies that these larvae can change their vertical distribution under certain dynamic conditions; I do not know of other nondecapod late-stage benthic invertebrate larval taxa that exhibit these patterns. This phenomenon is significant, because it suggests that this and other fronts, such as upwelling relaxation fronts or other buoyancy-driven onshore flows (e.g., Checkley et al. 1988; Farrell et al. 1991), may also be capable of transporting some deep larvae. This also implies that vertical distribution in nontransporting conditions may be a poor indi-

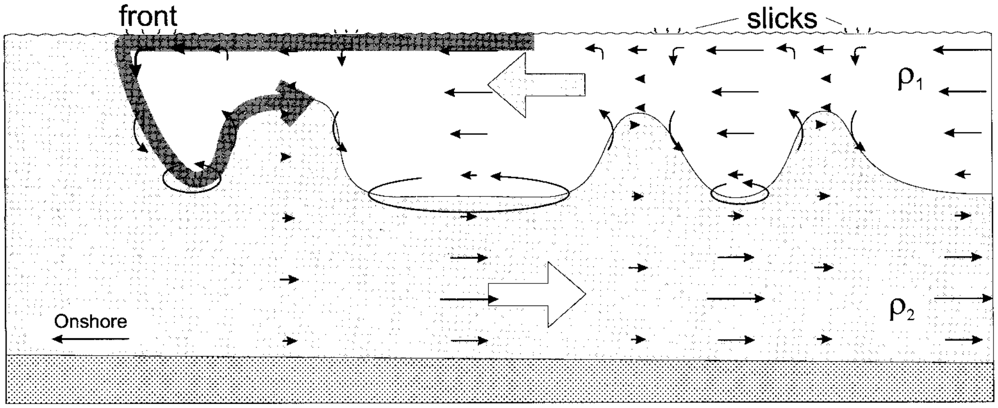

Fig. 14. Schematic model of circulation in internal bore warm fronts. The long, thick arrow at the surface illustrates the conveyor belt analogy. Short, thick arrows represent mass transport, thin arrows represent circulation, and ρ represents density. The shaded area would correspond, for example, to the subthermocline water in Fig. 8, the temperature of which is less than $\sim$19.4°C, and the nonshaded area would correspond to waters, the temperature of which is more than $\sim$19.4°C.

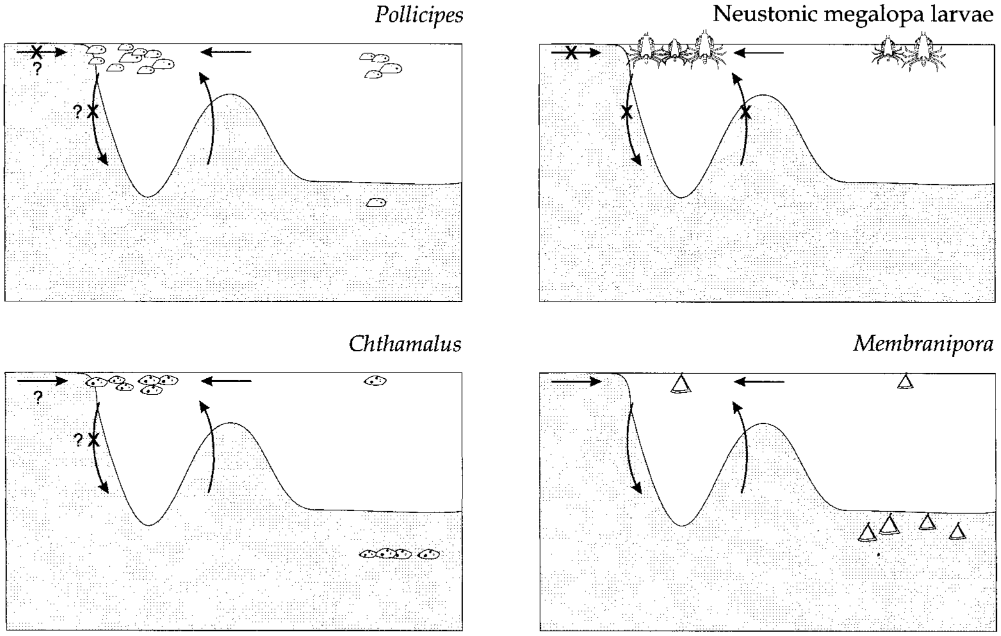

Fig. 15. Schematic representation of hypotheses for larval accumulation for *Pollicipes,* large neustonic crab larvae (Pineda 1994), *Chthamalus,* and *Membranipora.* Arrows represent likely larval pathways, crossed arrows represent unlikely pathways, and (?) represents a higher degree of uncertainty. Larvae to the right of the panels depict hypothesized vertical distributions from observations on the offshore side of the fronts.

cator of vertical distribution during transport and that vertical distributions in normal conditions should not be used to predict distributions in transporting conditions (e.g., Pineda 1991). This shift in vertical distribution is the result of both behavior and hydrodynamics: the result of behavior because other taxa with similar vertical distribution, such as *Membranipora,* did not accumulate and the result of hydrodynamics because high concentrations were found only at the convergences.

Larval concentration in the warm bore fronts is a critical phenomenon, because only those larvae that concentrate would transport onshore and recruit to the adult population. What could account for different patterns of concentration? (1) The observed circulation and the concentration of floating material at the fronts suggest that currents are capable of concentrating neustonic larvae such as crab megalopa. Neustonic larvae offshore of the front could concentrate at the front if currents behind the front would transport them toward the front (Fig. 15). (2) *Pollicipes* were not strictly neustonic, but abundances peaked at the sea surface on the offshore side of the fronts. Such larvae may also be transported toward the front by the surface currents behind the front (Fig. 15). (3) For the deeper dwelling *Chthamalus,* upwelling currents behind the fronts or in front of the crest of the high-frequency motions could entrain some larvae to the surface. These larvae could then be transported toward the front by the surface currents behind the front. However, because this taxon was also found on the onshore cold side of the fronts, the origin of frontal larvae could also be the waters in the cold side of the front. For frontal cyprids originating on the onshore cold side of the fronts, the front would collect the cyprids as it propagates (Fig. 15). The question of the origin of *Chthamalus* frontal larvae requires careful measurements of c, u at the sea surface, and larval concentrations in both sides of the front.

For accumulation at the front's surface, larvae would have to remain at the surface in spite of the front's downwelling currents. Both *Chthamalus* and *Membranipora* larvae were generally more abundant at 4 m than at the surface, *Chthamalus* in all sites but the front, and *Membranipora* in all but one offshore warm site. While *Chthamalus* accumulated at the front in three events, *Membranipora* did not. *Membranipora* is a weak swimmer that may be unable to withstand frontal downwelling currents (Fig. 15).

On 3 July 1996, larval frontal concentration was the lowest of all events, and observed c was the highest, suggesting that low concentration may have been the result of a very small difference between u and c. On the other hand, events such as the July 7 one, during which both *Chthamalus* and *Pollicipes* were highly concentrated, may have been the result of $u \gg c$. No physical observations are available, however, to contrast this hypothesis.

Origin of frontal larvae—Frontal larvae could originate onshore and offshore of the front. Intuitively, if surface larval concentration on the onshore cold and offshore warm side of the front are, respectively, L_c and L_w (in units larvae cm^{-3}) for frontal larvae originating mostly from the onshore side of the fronts, $u < c$, whereas for larvae originating mostly from the offshore warmer side of the fronts, $u \gg c$ and $L_w \gg L_c$. Assume a front advancing onshore with phase speed c (cm s^{-1}), cross-frontal distance is D_{f1} (cm), frontal

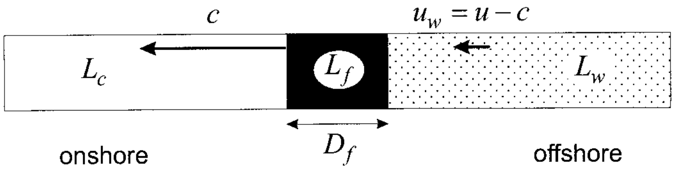

Fig. 16. Schematic representation of frontal concentration processes. c is phase speed; u is surface onshore currents offshore of the front; u_w is the speed at which offshore surface water approaches the front; D_f is cross-frontal distance; and L_c, L_f, and L_w are onshore, frontal, and offshore larval concentrations, respectively.

larval concentration is L_{f1} (larvae cm^{-3}), and the time necessary for accumulating the larvae is t (s) (Fig. 16). If all larvae encountered by the front are taken and retained, the density of larvae in the frontal zone is given by the following equation:

$$L_{f1}D_{f1} = L_c c t \tag{6}$$

Now assume another case in which larvae approach from offshore of the front, implying that $u > c$, L_{f2} is frontal larval concentration, and D_{f2} is cross-frontal distance. Assume that $u_w = u - c$ (cm s^{-1}) is the speed at which offshore surface water approaches the front, where u is surface onshore currents offshore of the front. Assuming that frontal larvae originate offshore of the front, larval density in the frontal zone is given by the equation

$$L_{f2}D_{f2} = L_w u_w t \tag{7}$$

Assuming that larvae approaching onshore and offshore yield the same larval density, then

$$L_{f1}D_{f1} = L_{f2}D_{f2} \tag{8}$$

and

$$L_c c = L_w u_w. \tag{9}$$

Equation 9 can be used to derive a criterion for the proportion of larval concentration L_c to L_w that must be met for the mechanisms of frontal larvae originating onshore or offshore of the front to be equally plausible. c is expected to be larger than u_w, and for the two mechanisms to be equally likely, $L_c < L_w$ by a factor of u_w/c.

This criterion can be used to explore the plausibility of larvae originating onshore or offshore of the front using the *Pollicipes* data. This exercise is speculative, as surface currents u were not measured, and larval and circulation observations did not coincide in two out of three cases. Only on 29 June 1996 was current speed u_b faster than phase speed c. u_b can be taken as a proxy for u, and $u = 17.6$, $c = 14.1$, and $u_w = 3.5$ cm s^{-1}. It follows that

$$\frac{L_c}{L_W} = \frac{3.5}{14.1} \approx \frac{1}{4} \tag{10}$$

Pollicipes larval abundances were 82, 4, 13, 44, and 5 on the offshore side closest to the fronts in the five sampling dates. Assuming the ¼-factor for both mechanisms to be equally likely of producing similar L_f, abundances in the onshore water need to be 20.5, 1, 3.25, 11, and 1.25. On the other hand, the abundances onshore of the front were 3, 3, 0, 0, and 0. The statistical hypothesis that larval abundance onshore = ¼ of larval abundance offshore (site closest to the front) was tested with a Scheirer–Ray–Hare nonparametric test (*see above*). Offshore larval abundances were multiplied by ¼, date was used for blocking, and abundance for each depth within a site and date were used as replicates (e.g., for 7 July 1996 at the onshore site, abundances for 0, 1, 2, and 4 m conform one group). Results show evidence of significant statistical difference ($P < 0.001$) for sites, with no evidence of statistical difference for dates. This result should be taken with caution; it only suggests that (1) if $u_w/c = ¼$ on the sampling dates and (2) if abundances for different depths can be taken as replicates, it is then likely that the origin of frontal *Pollicipes* larvae was offshore the fronts, not onshore.

The question of the origin of frontal larvae may be species dependent. Larvae originating onshore of the front should occur there. *Chthamalus* larvae are good candidates, because they were more abundant at depth and they occurred onshore of the front. On the other hand, strictly neustonic larvae with an extended larval period, such as the neustonic megalopa of *Pachygrapsus crassipes,* would have little probability of originating in the onshore cold side of the front, because after several weeks in the plankton, most of these larvae must be found offshore, and because the upwelled water on the onshore side has only a short residence time at the surface (e.g., ~6 h; Fig. 4), thus diminishing the probability of horizontal diffusion across the front from offshore waters to surface nearshore waters. This suggests that the origin of strictly neustonic frontal larvae would likely be offshore of the fronts rather than onshore. Observations of neustonic crab larvae in five events yielded no larvae on the cold side of the front, with most concentrated in the fronts and a few found on the offshore side (Pineda 1994). This suggests that these larvae originated on the offshore side of the front, which agrees with $u > c$.

An example of an accumulation mechanism by which organisms originate onshore of a propagating front is given by Franks (1997), who discussed ''ageostrophic'' fronts followed by surface bands that transported a red tide shoreward. Other than a photograph, no observations were reported. Although it is stated that ''the dynamics behind the front formation are unknown,'' internal bore fronts previously explained by Pineda (1994) were observed exactly in the same location, had the same periodicity and features, and were also correlated with red tides (Tynan 1993). The explanation of accumulation in those fronts is based on a simple model that assumes that the main source of particles ''is the near surface water in the path of the front.'' My results show that on 5, 7, and 19 July 1996, the taxa most concentrated in the fronts, *Pollicipes,* had no abundance at the onshore side of the fronts, where the source of particles would originate according to the model. For those dates, it is unlikely that frontal larvae originated at the onshore side of the front (also *see above*). However, for 1 and 3 July 1996 and also for *Chthamalus,* larvae were found onshore and offshore of the front, and the accumulation mechanism invoked by Franks (1997) may have worked in this instance. If this or other similar mechanisms that assume origin on the cold side operate in field conditions, even low abundances on the onshore side of the front may produce high concentration, because the front is approaching the onshore larvae at a speed c, whereas in the conveyor belt hypothesis invoked above, the larvae would approach the front at a speed $u - c$. Franks's (1997) model also explains accumulation in bands observed behind the front as a process that is different from internal wave slicks. Figures 8 and 9 show energetic internal waves, and field observations show slicks corresponding to these internal waves following the fronts. Bands following the fronts are then associated with high-frequency internal waves, and it is thus unnecessary to invoke other mechanisms for generating the surface banding.

Larval transport by internal waves—This study may help clarify the hypothesis of onshore transport of neustonic larvae by surface slicks over internal waves (Shanks 1983; Kingsford and Choat 1986; Shanks 1986). Surface slicks were often observed, and there was some concentration of surface material on those slicks. Those slicks most likely corresponded to the trailing side of the crest of the high-frequency internal motions, as found by Ewing (1950). The slicks were superimposed on the onshore surface flow (Fig. 6), resulting in slick and concentrated material that drifted shoreward with the bore flow (Pineda 1994). This scenario would explain the results of Shanks (1983, 1986) and Kingsford and Choat (1986), who were unaware of the warm bore phenomenon (Pineda 1994). The explanations differ slightly, however, because here the mechanism responsible for the transport of larvae would be the bore flow, not the slicks themselves. On the other hand, transport by slicks in the absence of the bores may also occur for fast-swimming taxa (Shanks 1995*b*; Lamb 1997). The swimming speeds required by Lamb's model appear to be too great for the small larvae considered in this study, but large decapod larvae could probably reach those speeds. Shanks's and Lamb's hypotheses require testing in field conditions, in an experiment in which the bore gravity flow is absent, the internal waves measured, and the circulation observed.

Conclusions

The hypothesis that frontal larvae originate offshore of a shoreward propagating front is based on observational and indirect evidence. However, this hypothesis requires further testing in the field and in the laboratory; only in one event was there evidence that $u > c$, and in this event, the vertical structure of the currents was different from that seen in the two other events. u must be measured close to the sea surface, as observed velocity profiles suggest that only there is it likely that $u > c$. My results show clear evidence of larval accumulation by warm bore fronts, but accumulation does not imply transport. On the other hand, if (1) larvae concentrate in the fronts, (2) larvae remain in fronts, and (3) fronts propagate all the way to the shore, this study would also show evidence of shoreward transport. The plausibility of points 1 and 2 is suggested by this study, while Pineda's (1994) results support points 1, 2, and 3, as kelp paddies and other debris transported in these bore fronts were later found in the surf zone. If kelp paddies and debris remain in the fronts, larvae too could remain in the fronts. Fronts are sites of intense biological and physical activity (Le Fèvre 1986). Internal bore warm fronts change the nutrient environment, transport mass in a direction perpendicular to the coastline, and have been observed transporting larvae onshore. Their dynamics are thus important in understanding the ecology of nearshore ecosystems.

References

ARTHUR, R. S. 1954. Oscillations in sea temperature at Scripps and Oceanside piers. Deep-Sea Res. **2:** 129–148.

BARNETT, A. M., AND A. E. JAHN. 1987. Pattern and persistence of a nearshore planktonic ecosystem off Southern California. Continental Shelf Res. **7:** 1–25.

CAIRNS, J. L. 1967. Asymmetry of internal tidal waves in shallow coastal waters. J. Geophys. Res. **72:** 3563–3565.

CHECKLEY, D. M., S. RAMAN, G. L. MAILLET, AND K. M. MASON. 1988. Winter storm effects on the spawning and larval drift of a pelagic fish. Nature (Lond.) **335:** 346–348.

ECKMAN, J. E. 1996. Closing the larval loop: Linking larval ecology to the population dynamics of marine benthic invertebrates. J. Exp. Mar. Biol. Ecol. **200:** 207–237.

EWING, G. C. 1950. Relation between band slicks at the surface and internal waves in the sea. Science **111:** 91–94.

FARRELL, T. M., D. BRACHER, AND J. ROUGHGARDEN. 1991. Cross-shelf transport causes recruitment to intertidal populations in central California. Limnol. Oceanogr. **36:** 279–288.

FRANKS, P. J. S. 1997. Spatial patterns in dense algal blooms. Limnol. Oceanogr. **42(5):** 1297–1305.

HELFRICH, K. R. 1992. Internal solitary wave breaking and run-up on a uniform slope. J. Fluid Mech. **243:** 133–154.

HOLLOWAY, P. E. 1987. Internal hydraulic jumps and solitons at a shelf break region on the Australian North West shelf. J. Geophys. Res. **92:** 5405–5416.

———. 1991. On the dissipation of internal tides, p. 449–468. *In* B. B. Parker [ed.], Tidal hydrodynamics. Wiley.

KINGSFORD, M. J., AND J. H. CHOAT. 1986. Influence of surface slicks on the distribution and onshore movements of small fish. Mar. Biol. (Berl.) **91:** 161–171.

LAMB, K. 1997. Particle transport by nonbreaking, solitary internal waves. J. Geophys. Res. **102:** 18641–18660.

LE FÈVRE, J. 1986. Aspects of the biology of frontal systems. Adv. Mar. Biol. **23:** 163–299.

———, AND E. BOURGET. 1992. Hydrodynamics and behaviour: Transport processes in marine invertebrate larvae. Trends Ecol. Evol. **7:** 288–289.

LEE, O. S. 1961. Observations on internal waves in shallow water. Limnol. Oceanogr. **6:** 312–321.

LEICHTER, J. J., G. SHELLENBARGER, S. J. GENOVESE, AND S. L. WING. 1998. Breaking internal waves on a Florida coral reef: A plankton pump at work? Mar. Ecol. Prog. Ser. **166:** 83–97.

———, S. L. WING, S. L. MILLER, AND M. W. DENNY. 1996. Pulsed delivery of sub-thermocline water to Conch Reef, Florida keys by internal tidal bores. Limnol. Oceanogr. **41:** 1490–1501.

PINEDA, J. 1991. Predictable upwelling and the shoreward transport of planktonic larvae by internal tidal bores. Science **253:** 548–551.

———. 1994. Internal tidal bores in the nearshore: Warm-water fronts, seaward gravity currents and the onshore transport of neustonic larvae. J. Mar. Res. **52:** 427–458.

———. 1995. An internal tidal bore regime at nearshore stations along western USA: Predictable upwelling within the lunar cycle. Continental Shelf Res. **15:** 1023–1041.

RICKETTS, E. F., AND J. CALVIN. 1968. Between Pacific tides, 4th ed. Stanford Univ. Press.

ROTHLISBERG, P. C., J. A. CHURCH, AND C. B. FANDRY. 1995. A mechanism for near-shore concentration and estuarine recruitment of post-larval *Penaeus plebejus* Hess (Decapoda, Penaeidae). Estuar. Coast. Shelf Sci. **40:** 115–138.

SCHELTEMA, R. S. 1986. On dispersal and planktonic larvae of benthic invertebrates: An eclectic overview and summary of problems. Bull. Mar. Sci. **39:** 290–322.

SHANKS, A. L. 1983. Surface slicks associated with tidally forced internal waves may transport pelagic larvae of benthic invertebrates and fishes shoreward. Mar. Ecol. Prog. Ser. **13:** 311–315.

———. 1986. Tidal periodicity in the daily settlement of intertidal barnacle larvae and an hypothesized mechanism for the cross-shelf transport of cyprids. Biol. Bull. (Woods Hole) **170:** 429–440.

———. 1995*a*. Mechanisms of cross-shelf dispersal of larval invertebrates and fish, p. 323–367. *In* L. McEdward [ed.], Ecology of marine invertebrate larvae. CRC.

———. 1995*b*. Oriented swimming by megalopae of several eastern North Pacific crab species and its potential role in their onshore migration. J. Exp. Mar. Biol. Ecol. **186:** 1–16.

SIMPSON, J. E. 1982. Gravity currents, in the laboratory, atmosphere, and ocean. Annu. Rev. Fluid Mech. **14:** 213–234.

———. 1997. Gravity currents: In the environment and the laboratory, 2nd ed. Cambridge Univ. Press.

———, AND R. E. BRITTER. 1979. The dynamics of the head of a gravity current advancing over a horizontal surface. J. Fluid Mech. **94:** 477–495.

SOKAL, R. R., AND F. J. ROHLF. 1995. Biometry, 3rd ed. Freeman.

STONER, A. W., R. A. GLAZER, AND P. J. BARILE. 1996. Larval supply to queen conch nurseries: Relationships with recruitment process and population size in Florida and the Bahamas. J. Shellfish Res. **15:** 407–420.

THORSON, G. 1950. Reproductive and larval ecology of marine bottom invertebrates. Biol. Rev. Camb. Philos. Soc. **25:** 1–45.

TYNAN, C. 1993. The effects of small-scale turbulence on dinoflagellates. Ph.D. thesis, Univ. of California–San Diego.

UFFORD, C. W. 1947. Internal waves measured at three stations. Trans. Am. Geophys. Union **28:** 87–95.

WINANT, C. D. 1974. Internal surges in coastal waters. J. Geophys. Res. **79:** 4523–4526.

———, AND A. BRATKOVICH. 1977. Structure and mixing within the frontal region density of a density current. Sixth Australasian Hydraulics and Fluid Mechanics Conference, Adelaide, Australia. p. 71–86.

———, AND ———. 1981. Temperature and currents in the Southern California shelf: A description of the variability. J. Phys. Oceanogr. **11:** 71–86.

———, AND J. R. OLSON. 1976. The vertical structure of coastal currents. Deep-Sea Res. **23:** 925–936.

YOSHIOKA, P. M. 1982. Role of planktonic and benthic factors in the population dynamics of the bryozoan *Membranipora membranacea*. Ecology **63:** 457–468.

Received: 2 April 1998
Accepted: 30 April 1999
Amended: 10 May 1999